Visualizing near-field coupling in terahertz dolmens

Alexei Halpin,[1,a)] Christiaan Mennes,[2] Arkabrata Bhattacharya,[1] and Jaime Gómez Rivas[1,3]
[1]*DIFFER - Dutch Institute for Fundamental Energy Research, De Zaale 20, 5600 HH, Eindhoven, Netherlands*
[2]*Center for Nanophotonics, AMOLF, Science Park 104, 1098 XG Amsterdam, Netherlands*
[3]*Department of Applied Physics, Eindhoven University of Technology, Postbus 513, 5600 MB, Den Dolech, Netherlands*

(Received 22 November 2016; accepted 22 February 2017; published online 8 March 2017)

Strong interactions between resonant structures in the near-field occur at length scales shorter than the wavelength, and can be exploited for modifying the propagation of electromagnetic radiation. Dolmen-like structures, formed by a rod supporting a dipolar (bright) resonance and two orthogonal rods with a quadrupolar (dark) resonance at the same frequency, represent a geometry of significant interest for near-field electromagnetic coupling. These structures demonstrate electromagnetically induced transparency (EIT) through coupling between these resonances, concurrently providing a sharp spectral selectivity in transmission and large group velocity reduction. We use near-field terahertz scanning microscopy to map the electric fields in the vicinity of a metallic dolmen in both amplitude and phase. In this way, we directly measure the interaction between bright and dark modes in the time-domain, revealing the physics resulting in EIT. We experimentally demonstrate the hybridization of bright and dark modes accompanying the near-field coupling, as well as the excitation of the dark mode at the frequency of the far-field transparency. [http://dx.doi.org/10.1063/1.4978031]

Resonant scatterers provide useful building blocks for designing components to manipulate terahertz (THz) radiation as an alternative to conventional optics. By exploiting the strong scattering properties of these structures, it is possible to fabricate THz modulators, filters, and beam routing elements,[1–6] where the thickness of the devices is a fraction of the wavelength.[7] Such devices can eventually be inserted into emerging implementations of THz optical communications[8] and imaging[9] systems, where the small footprints afforded by resonant structures are appealing in applications. Scattering structures, however, often consist of multiple elements placed in close proximity to one another, where near-field interactions between their constituent elements become important.[10,11] Near-field coupling presents the benefit of allowing further manipulation of the scatterers spectral behaviour, but demands near-field microscopy for full device characterization since the link from near-field properties to far-fields is not always direct.[12,13]

In this manuscript, we present a study on a dolmen structure, consisting of a horizontal rod and two orthogonal vertical rods, where the near-field coupling leads to electromagnetically induced transparency (EIT).[14,15] The horizontal rod is oriented along the polarization of the incident field and supports a bright mode, while the vertical rods support a dark mode. Coupling between these modes results in the appearance of a sharp peak in the transmission spectrum (or dip in extinction) accompanied by a large group velocity dispersion, with potential applications in sensing or information processing.[16,17]

At optical frequencies, near-field measurements on plasmonic dolmens using near-field scanning optical microscopy[18] and electron microscopy[19] have previously shown signatures of the bonding and antibonding resonances that arise in the coupled system[20] as illustrated in Fig. 1(a). Nevertheless, in spite of the impressive spatial resolutions achieved by these techniques, they are restricted to measuring only the intensity distributions unless combined with interferometry.[21]

In contrast, at THz frequencies, it is possible to directly measure the time-dependent electric near-fields of resonant metallic structures.[22–24] Over recent years, a number of innovative advances have emerged in near-field THz microscopy resulting in diverse implementations, ranging from techniques based on sharp tips[25,26] or electron pulses[27] for ultra-high spatial resolution, to others harnessing electro-optic sampling in nonlinear crystals,[28,29] to schemes based on miniaturized photoconductive probes.[13,30,31] We employ the latter approach to demonstrate the hybridization of modes that follows the near-field coupling between two resonant structures, as well as the excitation of the dark resonance which is responsible for the transparency window in the far-field.

The dolmens presented here can be described as follows: a resonant structure, here a gold rod oriented along the polarization of the incoming radiation, is placed in close vertical proximity to a pair of orthogonally oriented rods which constitute the second resonator. The top rod supports a bright dipolar-like ($\lambda/2$ resonance) which couples to free-space radiation. The driving field induces a dipole field in the metallic rod, which for very short distances is dominated by the near-field component. For a homogeneous environment, this field takes the form[32]

$$\mathbf{E}(\mathbf{r}) = \frac{1}{4\pi\epsilon_0}\left[3\mathbf{n}(\mathbf{n}\cdot\mathbf{p}) - \mathbf{p}\right]\frac{1}{r^3}, \tag{1}$$

where r denotes the distance from the centre of the dipole, $\mathbf{p}$ denotes the dipole moment, and $\mathbf{n}$ is the radial unit vector. The dipolar resonance is spectrally very broad due to its

a)Electronic mail: a.halpin@differ.nl

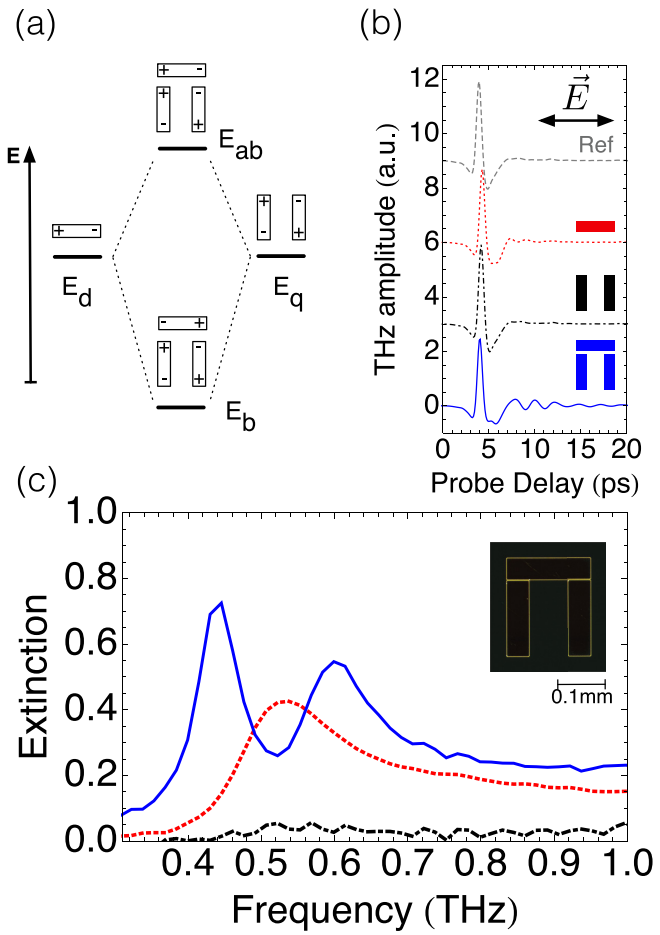

FIG. 1. (a) Illustration of the formation of hybrid modes as a result of near-field coupling in a dolmen: E_d, E_q, E_b, and E_{ab} represent the energies of the dipolar, quadrupolar, bonding, and antibonding resonances, respectively. (b) Measured THz transients transmitted through the substrate (grey, dashed), a random array of dipolar rods (red, dotted), of quadrupolar rod pairs (black, dot-dashed), and of dolmens (blue, solid). (c) Extinction measurements corresponding to transients in panel (b), where the filling fractions are 5%, 12%, and 12% for the dipolar rods, quadrupolar rods, and dolmens, respectively. The frequency resolution is 15 GHz. Inset: dark-field microscope image of dolmen at 20× magnification).

short lifetime originating from large radiative losses. However, when the vertical rod pair is brought into close proximity with the dipolar rod, the near-fields described by Eq. (1) will subsequently drive similar $\lambda/2$ resonances in each of the vertical rods. In this way, the asymmetry of the structure is used to access a dark mode,[33] as has been exploited previously for the generation of high-Q resonances for metamaterials,[34] and sensing applications.[35,36] The antisymmetric field about the midpoint of the dipolar rod, dictates that each of the vertical rods will be driven out-of-phase with respect to each other. Therefore, the vertical rods taken together support a resonance with a quadrupolar character at a similar frequency to that of the dipolar resonance. Symmetry dictates that this resonance also does not directly couple to free-space radiation, which accounts for why the resonance is dark and spectrally narrow, from the absence of radiative losses.

The structures are composed of gold with 100 nm thickness, and were fabricated following standard photolithography procedures on quartz substrates. The dipolar rod has a length of 150 μm and a width of 40 μm, while the rods comprising the quadrupolar pair have a length of 140 μm and a width of 40 μm. A dark-field microscope image of one dolmen is shown in the inset of Fig. 1(c). We prepared arrays of structures arranged in a random fashion to characterize the resonances supported by the samples using far-field spectroscopy. The spectra are collected using a commercial THz time domain spectroscopy (TDS) setup (Menlo Systems GmbH), with results shown for arrays having filling fractions ranging from $\sim$7–20% corresponding to the total area covered by metal.

In Fig. 1(b), the THz transients for the substrate (grey, dashed) and quadrupolar rods (black, dot-dashed) are very similar for this polarization, demonstrating the absence of coupling to incident radiation by the quadrupolar mode. On the other hand, the transient associated with the sample of dipolar rods (red, dotted) exhibits an overdamped resonance corresponding to the excitation of the aforementioned $\lambda/2$ resonance. For the dolmen sample (blue, solid), the transient displays an underdamped component arriving at delayed times corresponding to the sample becoming transmissive as a result of the coupling between the two resonators.

By Fourier transformation of these transients and referencing to the transmission of the bare substrate, we compute the intensity extinction spectra for the samples as shown in Fig. 1(c). The sample of dipolar rods supports a strong and broad resonance centered at $\nu = 0.54$ THz, while for the quadrupolar rod pair, we observe a featureless far-field spectrum with negligible extinction. The quadrupolar mode supported by the structures cannot couple with the orthogonal polarization used here, and the $\lambda/2$ resonance along their width lies outside the frequency range of interest. For the dolmen structures, we observe a splitting of the bright mode into two peaks corresponding to bonding and antibonding modes,[18] with a reduced extinction at what was previously the frequency of maximum extinction for the bright mode. This reduced extinction or EIT results from the interference between bright and dark modes, and can be described classically with a coupled oscillator model.[37] To support the assignment of these modes, and to ascertain the near-field distributions giving rise to the transparency observed in Fig. 1(c), we probe an isolated dolmen in a near-field microscope. Here a separate, previously described[13,38] experimental setup is used, based on a THz near-field probe (TD-800-Z-WT, Protemics GmbH, Germany) with a lateral spatial resolution in the order of 10 μm.[30] The electric field $E_z(t)$ is measured across the sample by raster-scanning the near-field probe at a height of 1 μm above the sample. The temporal evolution of the polarization induced in the dolmen is therefore collected over the full area surrounding the structure. Afterwards, Fourier transformation of each measured THz transient allows to recover the spatial near-field maps both in amplitude and phase.

The results of these scans for a dolmen with a 1 μm gap separating bright and dark resonators are shown in Fig. 2, where we plot the real part of E_z. Beginning with the maps for $\nu = 0.47$ THz in Fig. 2(a), the near-fields in the top rod assume a dipolar field distribution corresponding to the $\lambda/2$ resonance of the rod. Similarly, the rods in the quadrupolar resonator also exhibit dipolar field distributions, with opposite phases in each rod, revealing the overall quadrupolar

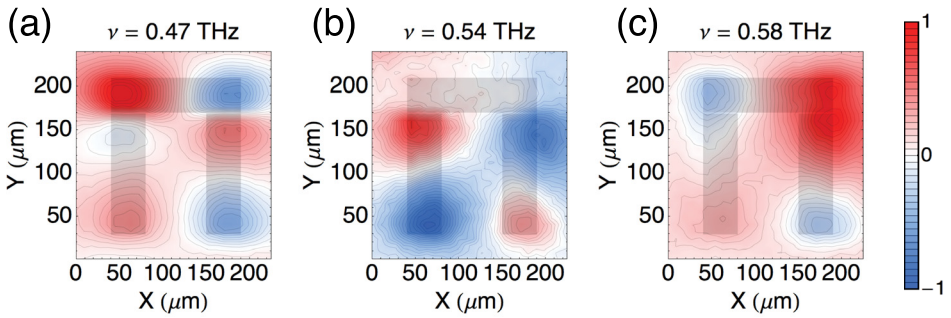

FIG. 2. Measured real part of the E_z component of the near-field, corresponding to an excited dolmen with a gap of 1 μm separating the bright and dark resonators at selected frequencies. Each spectral map is normalized to its own maximum value, corresponding to an overall scaling factor of unity for panel (a), 3.5 for panel (b), and 2 for panel (c). Contours given at 5%.

character for the dark mode. For this frequency, the relative phases of the electric field across the gap separating the resonators are opposite, giving rise to the so-called bonding mode corresponding to the lower energy resonance observed in the far-field. At $\nu = 0.54$ THz in Fig. 2(b), the near-fields surrounding the dipolar rod are suppressed, and are instead enhanced in the vicinity of the quadrupolar rod pair, consistently with the reduction of extinction observed in the far-field spectrum for those frequencies. Finally, at $\nu = 0.58$ THz in Fig. 2(c), we observe a change in the relative phase of the two resonators, corresponding to the antibonding mode where repulsive interactions between top and bottom resonators increase the resonance frequency.

The near-field maps for a gap of 1 μm demonstrate strong hybridization between the bright and dark resonances of the dolmens due to near-field coupling, as shown above. Increasing the gap size allows to tune the strength of the near-field coupling. Through fabrication of dolmens possessing larger gap sizes, we show in Fig. 3, the gap size dependence on the spectral features discussed thus far. In Fig. 3(a), the extinction spectrum highlights that near-field coupling becomes negligible for gap sizes on the order of 15 μm or larger, leading to unresolved bonding and antibonding modes and no induced transparency. For a gap size of 45 μm, the extinction already resembles that of the dipolar resonance.

By monitoring the peak locations of the hybrid modes in Fig. 3(b), we confirm that once the structures are brought to within a distance of approximately 15 μm, the effects of near-field coupling become important, and that for larger gaps, no hybridization takes place. As we show next, this distance over which the two coupled resonators will interact strongly can be understood from the spatial decay of the bright mode. In Fig. 3(c), we show the near-field spatial map corresponding to an isolated rod at the frequency of $\lambda/2$ resonance. This map indicates the spatial extent of the near-fields associated with the dipolar-like resonance supported by the rod. By taking a line profile across the width of the rod as in Fig. 3(d), we recover the decay of the electric field at the position where the quadrupolar rods are placed in the dolmen samples. We find that the field amplitude decays by approximately 80% relative to its maximal value within a 20 μm distance from the edge in the lateral direction. While this figure is in the order of the probe resolution, it is nonetheless consistent with the onset of splittings measured in the far-field spectra for those gap sizes. Moreover, full-wave simulations of our experiment using the commercial finite-domain time-

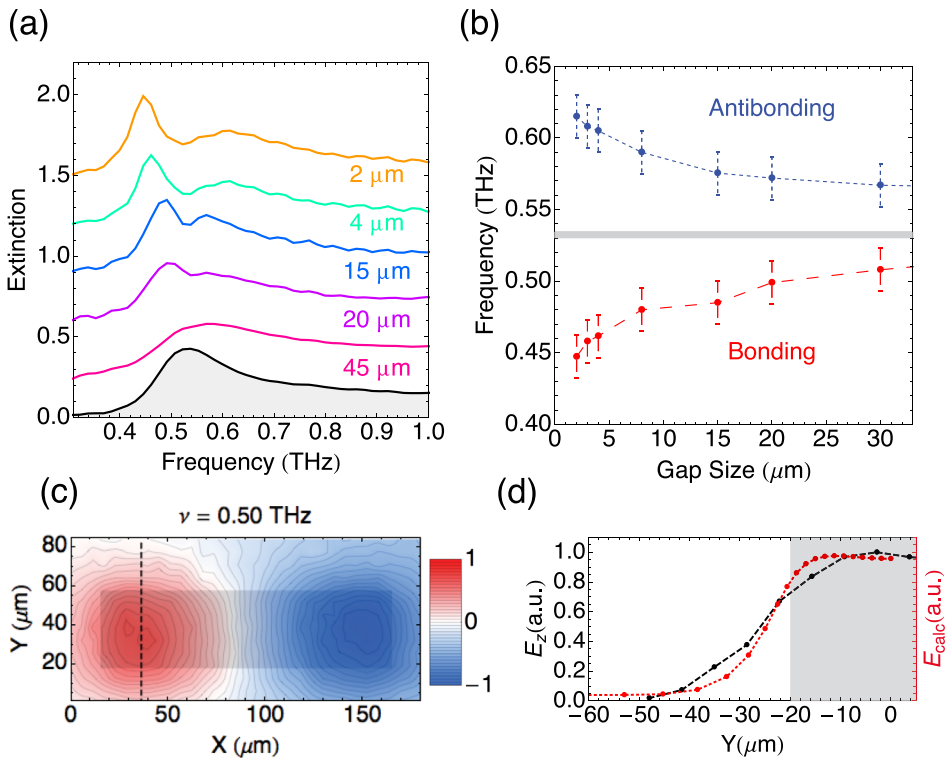

FIG. 3. (a) Extinction spectra of random arrays of dolmens (12% filling fraction) as a function of gap size, with traces shifted by 0.3. The extinction spectrum of the dipolar resonance is shown in black (grey filling). (b) Frequencies of bonding and antibonding modes as a function of gap size, with error bars given by the experimental frequency resolution. The grey line indicates the frequency of the dipolar resonance. (c) Near-field map of an isolated rod at the frequency of $\lambda/2$ resonance, contours given at 5% (rod is shown in grey overlay). (d) Line profile through the dashed line in (c), showing the decay of E_z along the Y-direction (black, dashed) along with a comparison to numerical simulations (red, dotted).

domain (FDTD) software predict similar decay profiles for the near-fields as those measured using the microprobes, as shown in the red trace of Fig. 3(d). For these simulations, we place a near-field monitor at a height of 10 μm above the substrate, corresponding to the physical height of the photoswitch in the microprobe.

In conclusion, using THz spectroscopy in both near- and far-fields, we have investigated EIT at THz frequencies in a gold dolmen structure. Near-field scanning microscopy was used to map out the field distributions of the modes which are formed via near-field coupling within the dolmen structure, where the bonding and antibonding modes, which arise due to hybridization of bright and dark resonances were revealed in both amplitude and phase. By varying the geometry of the structures, the coupling strength between bright and dark modes was tuned, with accompanying variation in hybridization and induced transparency. Moreover, near-field microscopy on the bright resonator reveals the minimum distance required for observation of effective coupling between bright and dark modes. These results highlight the underlying physics in this structure of two interacting resonators, resolving the coupling which gives rise to the transparency by measuring the near-field excitation of the dark mode at the frequency where extinction is suppressed in the far field.

We would like to acknowledge Niels Commandeur and Luc Blom for technical support. The authors would like to acknowledge funding via the ERC Grant Nos. 259272 THZ-PLASMON (2010) and 665619 MicroMap (2014).

[1]H. T. Chen, W. J. Padilla, J. M. O. Zide, A. C. Gossard, A. J. Taylor, and R. D. Averitt, Nature **444**, 597 (2006).
[2]V. Giannini, A. Berrier, S. A. Maier, J. A. Sánchez-Gil, and J. G. Rivas, Opt. Express **18**, 2797 (2010).
[3]M. Seo, J. Kyoung, H. Park, S. Koo, H. S. Kim, H. Bernien, B. J. Kim, J. H. Choe, Y. H. Ahn, H. T. Kim, N. Park, Q. H. Park, K. Ahn, and D. S. Kim, Nano Lett. **10**, 2064 (2010).
[4]L. Razzari, A. Toma, M. Shalaby, M. Clerici, R. P. Zaccaria, C. Liberale, S. Marras, I. A. I. Al-Naib, G. Das, F. De Angelis, M. Peccianti, A. Falqui, T. Ozaki, R. Morandotti, and E. Di Fabrizio, Opt. Express **19**, 26088 (2011).
[5]J. Gu, R. Singh, X. Liu, X. Zhang, Y. Ma, S. Zhang, S. A. Maier, Z. Tian, A. K. Azad, H. T. Chen, A. J. Taylor, J. Han, and W. Zhang, Nat. Commun. **3**, 1151 (2012).
[6]T. P. Steinbusch, H. K. Tyagi, M. C. Schaafsma, G. Georgiou, and J. G. Rivas, Opt. Express **22**, 26559 (2014).
[7]R. Singh, E. Smirnova, A. J. Taylor, J. F. O'Hara, and W. Zhang, Opt. Express **16**, 6537 (2008).
[8]I. F. Akyildiz, J. M. Jornet, and C. Han, Phys. Commun. **12**, 16 (2014).
[9]J. Grant, Y. Ma, S. Saha, A. Khalid, and D. R. S. Cumming, Opt. Lett. **36**, 3476 (2011).
[10]P. K. Jain and M. A. El-Sayed, Chem. Phys. Lett. **487**, 153 (2010).
[11]J. B. Lassiter, H. Sobhani, M. W. Knight, W. S. Mielczarek, P. Nordlander, and N. J. Halas, Nano Lett. **12**, 1058 (2012).
[12]B. Gallinet and O. J. F. Martin, Opt. Express **19**, 22167 (2011).
[13]A. Bhattacharya, G. Georgiou, S. Sawallich, C. Matheisen, M. Nagel, and J. Gómez Rivas, Phys. Rev. B **93**, 035438 (2016).
[14]S. Zhang, D. A. Genov, Y. Wang, M. Liu, and X. Zhang, Phys. Rev. Lett. **101**, 047401 (2008).
[15]N. Liu, L. Langguth, T. Weiss, J. Kästel, M. Fleischhauer, T. Pfau, and H. Giessen, Nat. Mater. **8**, 758 (2009).
[16]J. B. Khurgin, J. Opt. Soc. Am. B **22**, 1062 (2005).
[17]N. Liu, T. Weiss, M. Mesch, L. Langguth, U. Eigenthaler, M. Hirscher, C. Sönnichsen, and H. Giessen, Nano Lett. **10**, 1103 (2010).
[18]Z. Ye, S. Zhang, Y. Wang, Y. S. Park, T. Zentgraf, G. Bartal, X. Yin, and X. Zhang, Phys. Rev. B **86**, 155148 (2012).
[19]T. Coenen, D. T. Schoen, B. J. M. Brenny, A. Polman, and M. L. Brongersma, Phys. Rev. B **93**, 195429 (2016).
[20]S. C. Yang, H. Kobori, C. L. He, M. H. H. Lin, H. Y. Chen, C. Li, M. Kanehara, T. Teranishi, and S. Gwo, Nano Lett. **10**, 632 (2010).
[21]N. Ocelic, A. Huber, and R. Hillenbrand, Appl. Phys. Lett. **89**, 101124 (2006).
[22]M. A. Seo, A. J. L. Adam, J. H. Kang, J. W. Lee, S. C. Jeoung, Q. H. Park, P. C. M. Planken, and D. S. Kim, Opt. Express **15**, 11781 (2007).
[23]A. Bitzer and M. Walther, Appl. Phys. Lett. **92**, 231101 (2008).
[24]C. A. Werley, K. Fan, A. C. Strikwerda, S. M. Teo, X. Zhang, R. D. Averitt, and K. A. Nelson, Opt. Express **20**, 8551 (2012).
[25]K. Moon, H. Park, J. Kim, Y. Do, S. Lee, G. Lee, H. Kang, and H. Han, Nano Lett. **15**, 549 (2015).
[26]B. J. Bohn, M. Schnell, M. A. Kats, F. Aieta, R. Hillenbrand, and F. Capasso, Nano Lett. **15**, 3851 (2015).
[27]A. Ryabov and P. Baum, Science **353**, 374 (2016).
[28]R. I. Stantchev, B. Sun, S. M. Hornett, P. A. Hobson, G. M. Gibson, M. J. Padgett, and E. Hendry, Sci. Adv. **2**, e1600190 (2016).
[29]F. Blanchard and K. Tanaka, Opt. Lett. **41**, 4645 (2016).
[30]M. Wächter, M. Nagel, and H. Kurz, Appl. Phys. Lett. **95**, 041112 (2009).
[31]A. J. Macfaden, J. L. Reno, I. Brener, and O. Mitrofanov, Appl. Phys. Lett. **104**, 011110 (2014).
[32]J. Jackson, *Classical Electrodynamics* (Wiley, 1962).
[33]D. R. Chowdhury, X. Su, Y. Zeng, X. Chen, A. J. Taylor, and A. Azad, Opt. Express **22**, 19401 (2014).
[34]R. Singh, I. A. I. Al-Naib, Y. Yang, D. Roy Chowdhury, W. Cao, C. Rockstuhl, T. Ozaki, R. Morandotti, and W. Zhang, Appl. Phys. Lett. **99**, 201107 (2011).
[35]C. Debus and P. H. Bolívar, Appl. Phys. Lett. **91**, 184102 (2007).
[36]C. Wu, A. B. Khanikaev, R. Adato, N. Arju, A. A. Yanik, H. Altug, and G. Shvets, Nat. Mater. **11**, 69 (2011).
[37]C. L. Garrido Alzar, M. A. G. Martinez, and P. Nussenzveig, Am. J. Phys. **70**, 1 (2001).
[38]A. Bhattacharya and J. Gómez Rivas, APL Photonics **1**, 086103 (2016).